Princeton Plasma Physics Laboratory

PPPL-4099

PPPL-4099

2-D Reflectometer Modeling for Optimizing the ITER Low-field Side X-mode Reflectometer System

G.J. Kramer, R. Nazikian, E.J. Valeo, R.V. Budny,
C. Kessel, and D. Johnson

September 2005

PPPL
PRINCETON PLASMA
PHYSICS LABORATORY

Prepared for the U.S. Department of Energy under Contract DE-AC02-76CH03073.

PPPL Report Disclaimers

Full Legal Disclaimer

Trademark Disclaimer

PPPL Report Availability

This report is posted on the U.S. Department of Energy's Princeton Plasma Physics Laboratory Publications and Reports web site in Fiscal Year 2005. The home page for PPPL Reports and Publications is: http://www.pppl.gov/pub_report/

Office of Scientific and Technical Information (OSTI):

Available electronically at: http://www.osti.gov/bridge.

Available for a processing fee to U.S. Department of Energy and its contractors, in paper from:

U.S. Department of Energy
Office of Scientific and Technical Information
P.O. Box 62
Oak Ridge, TN 37831-0062

Telephone: (865) 576-8401

Fax: (865) 576-5728

E-mail: reports@adonis.osti.gov

National Technical Information Service (NTIS):

This report is available for sale to the general public from:

U.S. Department of Commerce
National Technical Information Service
5285 Port Royal Road
Springfield, VA 22161

Telephone: (800) 553-6847

Fax: (703) 605-6900

Email: orders@ntis.fedworld.gov

Online ordering: http://www.ntis.gov/ordering.htm

2-D reflectometer modeling for optimizing the ITER low-field side X-mode reflectometer system

G.J. Kramer,* R. Nazikian, E.J. Valeo, R.V. Budny, C. Kessel, and D. Johnson

Princeton Plasma Physics Laboratories,

P.O.box 451, Princeton, New Jersey 08543

(Dated: March 15, 2006)

Abstract

The response of a low-field side X-mode reflectometer system for ITER is simulated with a 2-D reflectometer code using a realistic plasma equilibrium. Relativistic corrections to the plasma permitivity due to the high electron temperature were included. It is found that the reflected beam will often miss its launch point by as much as 40 cm and that a vertical array of receiving antennas is essential in order to observe a reflection on the low-field side of ITER. Relativistic absorption effects were studied with a 1-D full wave code and found to be insignificant for reflections from the low-field side up to the plasma center.

*gkramer@pppl.gov

I. INTRODUCTION

Reflectometry is one of the key diagnostics for the International Thermonuclear Experimental Reactor (ITER) [1]. In the present design of the ITER tokamak there are three major reflectometer systems envisioned: a low-field side system, a high-field side system and a plasma position control system. A fourth reflectometer system in the divertor has so far been deemed technically too difficult to construct [2]. Once a diagnostic is installed on ITER access to it is extremely difficult due to the very harsh enviroment and ITER's size. Removing a port plug in which the diagnostics are mounted for maintenance is an expensive and time consuming operation and has to be avoided as much as possible. A good analogy for ITER diagnostics are instruments mounted on satellites in space. Once the satellite is launched there is no access to the instrument to correct flaws. For ITER diagnostics something similar holds: once the the diagnostic is launched in ITER-space (mounted on ITER) one normally does not have access to it any more for repairs and/or changes. Thus in the design phase of diagnostics for ITER it is of paramount importance to study and predict its response in relation to expected plasma scenarios in order to optimize the diagnostic and find possible weaknesses and correct them before building the diagnostics.

In this paper we study the behavior of the low-field side reflectometer system with a full wave 2-D reflectometer code, FWR2D [3]. The FWR2D code has been validated successfully against laboratory experiments [4, 5] and it has been applied to interpret reflectometer data that was taken on the JT-60U tokamak [6].

After discussing the used ITER target plasma in section II we study the relativistic effects due to the finite electron temperature on the reflection layers in section III. Upper X-mode reflectometer simulations are presented in section IV and based on those results an antenna system for the ITER low-field side reflectometer system is proposed in section V. This is followed by the conclusions in section VI.

II. ITER TARGET PLASMA

Various tools are being used for integrated modeling of ITER plasmas, including the rampup to steady conditions and rampdown to termination. One set of tools is a combination of the Tokamak Simulation Code (TSC) [7] with the GLF23 model [8] to predict the

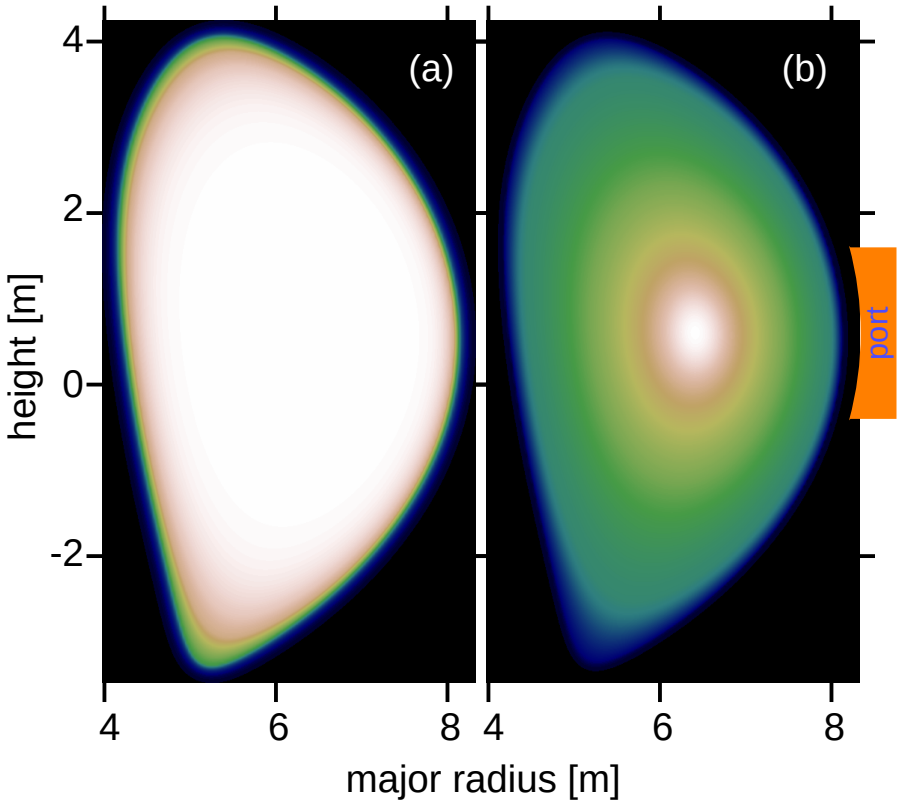

FIG. 1: color contour plot of (a) the electron density and (b) the electron temperature of the ITER plasma used in this paper. The maximum density, indicated in pink, is 6 10^{19}m^{-3} and the maximum temperature is 26.5 keV.

temperature evolution, and the TRANSP code [9] with detailed heating and current drive capabilities. ITER plasma regimes that have been modeled this way include amongst others the ELMy H-mode and the Hybrid regime. The Hybrid regime has a higher confinement than the ELMy H-mode and typically a magnetic safety factor at the plasma center that is larger than one. In the reflectometer simulations that follow we have used a Hybrid plasma at a time when the current has reached its flat top value of 15 MA and the density is still rising slowly. A cross section of the plasma with electron density and temperature contours is shown in Fig. 1. The plasma shape of ITER is up-down assymetric due to the divertor and as a consequence the flux surfaces at the mid-plane are in general not vertical but tilted slightly. in section IV we investigate the effects of this tilt on low field side reflectometry. The electron density profile is flat in the core with steep density gradients at the edge (see Fig. 2a). The edge region with the density gradients can only be probed with O-mode re-

flectometry. In this paper we aim to study the reflectometer response from different parts of the plasma, not only the edge, therefore we have performed our simulations using the upper X-mode reflection layer. The modulus of the magnetic field that is used in the simulations includes the contributions of the toroidal and poloidal magnetic fields and the diamagnetic effect. It is dominated by the toroidal magnetic field (Fig. 2b). Because the toroidal magnetic field is the dominant contribution to the modulus of the magnetic field which enters in the equation for the X-mode reflection layers it is expected that most parts of the plasma are accessible from the low field side with upper X-mode reflectometry for sufficiently low densities.

III. ELECTRON TEMPERATURE EFFECTS

The electron temperature which is shown in figs. 1b and 2c is high, up to 26.5 keV, and peaked at the plasma center. This has two effects on the operation of microwave reflectometer diagnostics: i) absorption of microwave power at the relativistically down-shifted second harmonic Electron Cyclotron Emission (ECE) layer and ii) relativistic corrections to the plasma permitivity. These two issues will be addressed in the following sub-sections.

A. absorption effects

The reflectometer system the absorption of microwave power in hot fusion plasmas can make it difficult to get sufficiently strong reflected signals back from reflection layers close to and beyond the hot plasma core. We have estimated the attenuation of the microwave power with a 1-D full wave code [4] in which we have used the weakly relativistic approximation for the dielectric tensor as given in [10, 11] for the plasma described in Sec. II at the plasma mid-plane. We have found that in this case the attenuation for a round-trip of the waves is less than 1 dB for microwaves reflecting off layers at the low-field side while the absorption of the microwave power that is reflected beyond the plasma center increases steeply as can be seen in Fig. 3. The reason for this steep increase is that the probing frequencies for those layers are close to the down-shifted second harmonic ECE frequency.

The microwave absorption for high-field side reflection becomes only significant for electron temperatures above 20 keV as can be seen from Fig. 3 where we have calculated the

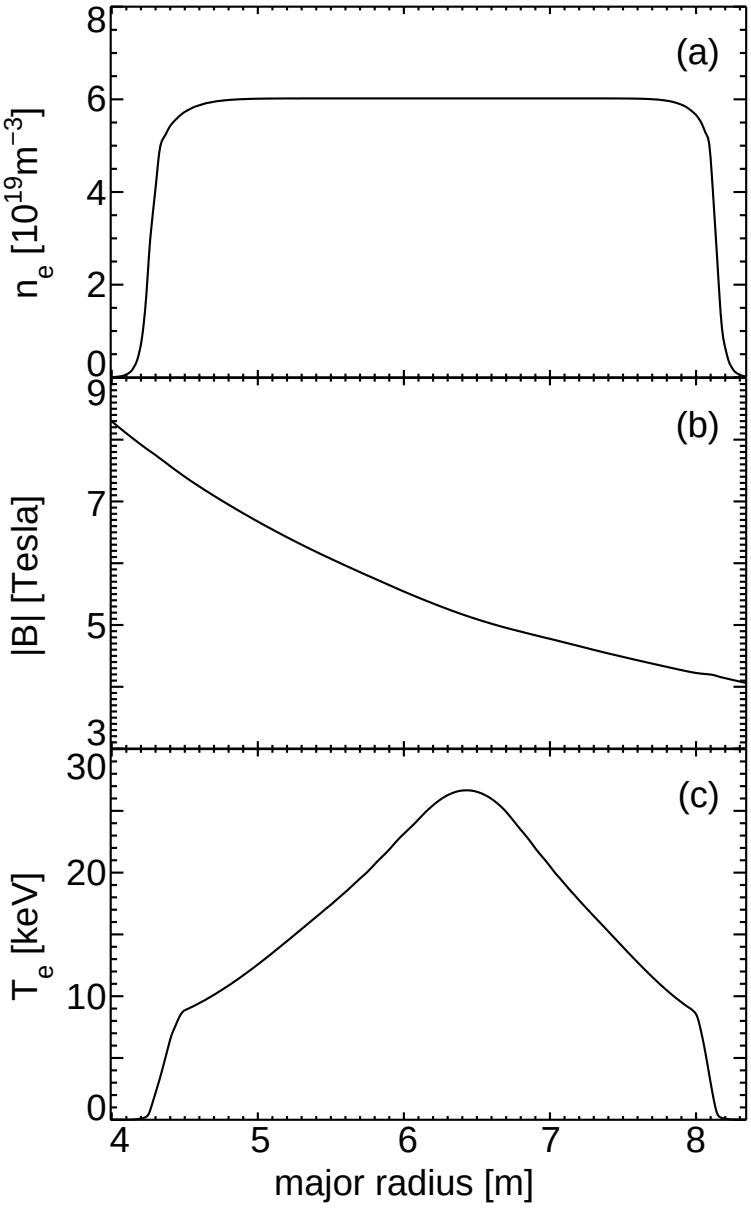

FIG. 2: The electron density (a), magnetic field (b), and electron temperature (c) at the plasma mid-plane.

round-trip absorption for 190 GHz microwaves for the profiles shown in Fig. 2 but with lower peak electron temperatures.

The absorption, however, does not affect the wave propagation in the plasma as calculated in the remainder of this paper with a 2-D code. The absorption should be included in the calculation of reflected power levels together with a full 3-D treatment of the microwave propagation. Estimating reflected power levels at the receiver antennas is therefore beyond

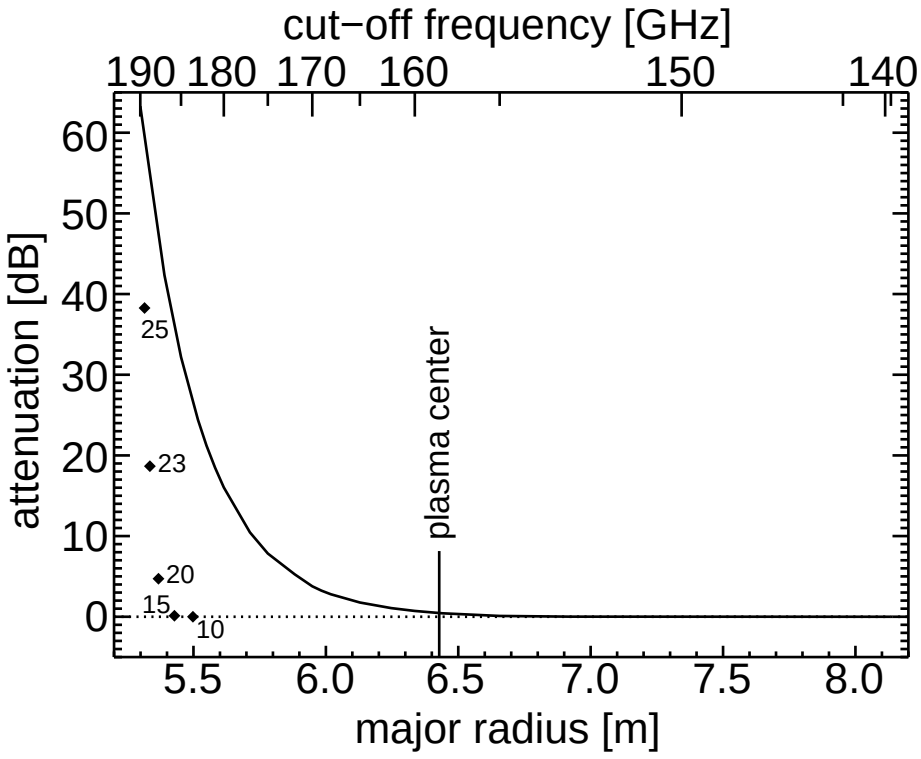

FIG. 3: Microwave absorption at the plasma mid-plane as a function of major radius (bottom scale) and X-mode cut-off frequency (top scale). For the hybrid scenario with a peak electron temperature of 26.7 keV. The absorption and reflection location for 190 GHz were also calculated calculated at lower peak electron temperatures and are indicated with the diamonds labeled with their peak electron temperature. Absorption effects for the ITER hybrid scenario become significant at the high-field side when peak electron temperatures rise above about 20 keV.

the scope of this paper.

B. relativistic plasma permitivity

In the cold plasma approximation the X-mode plasma permitivity is only a function of the electron density and the magnetic field strength. In fusion plasmas, however, relativistic effects due to the electron thermal velocity modify the plasma permitivity [12]. For plasmas in ITER where central electron temperatures are expected in the order of 15 to 30 keV relativistic corrections significantly modify the location of the reflection layers. The upper X-mode reflection layers are affected more strongly than the lower X-mode and O-mode

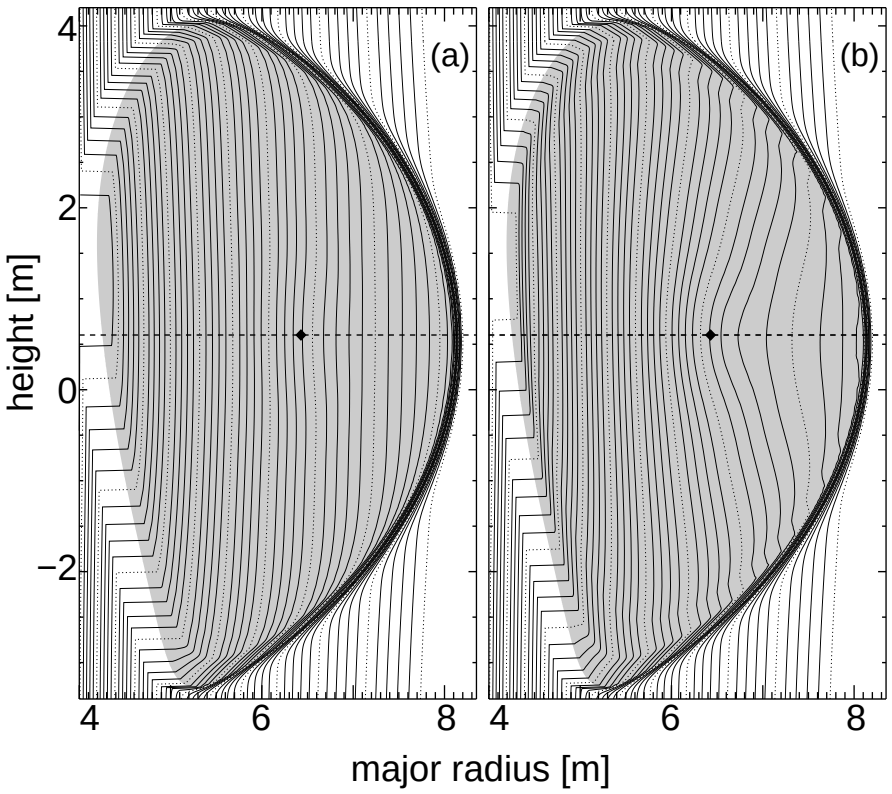

FIG. 4: Upper X-mode contours for a cold plasma ($T_e = 0$) (a) and for a hot plasma (b). The contours range from 120 GHz at the right in steps of 2 GHz while multiples of 10 GHz are indicated with dotted lines. The contour at the left is 232 GHz and 230 GHz for (a) and (b) respectively. The contour that passes through the plasma center (indicated with a diamond) is 172 GHz in (a) and 158 GHz in (b).

reflection layers [13].

We have calculated the upper X-mode reflection contours using the cold plasma approximation (Fig. 4a) and using a relativistic expression which takes into account the finite electron temperature (Fig. 4b). In these relativistic calculations we have used an effective electron mass, m_e^*, given in [11] as:

$$\frac{m_e^*}{m_e} = 3K_2(\mu)/\mu^2 \int_0^\infty \frac{p^4 \exp(-\mu\gamma)}{\gamma(\gamma - s\Omega)} \mathrm{d}p \tag{1}$$

with m_e the electron rest mass, p the electron momentum, $\mu = m_e \mathrm{c}^2/T_e$, T_e the electron temperature, $K_2(\mu)$ the modified Bessel function of the second kind, $\gamma = \sqrt{1+p^2}$, $\Omega = \omega_c/\omega_s$ the electron cyclotron frequency divided by the cut off frequency and $s = 1, 0, -1$ for the upper X-mode, O-mode, and lower X-mode cut off layer, respectively.

Because of the nearly constant density and the dominance of the toroidal magnetic field, the upper X-mode reflection layers form nice parallel mirrors if electron temperature corrections are neglected (Fig. 4a) and the reflected signals return back to the launch point. When electron temperature corrections are included, the reflection layers curve strongly (Fig. 4b) due to the peaked electron temperature profile. The returning waves are generally reflected to a location away from the transmitter antenna. In the next section we investigate where the reflected signals return to from these curved reflection layers.

IV. REFLECTOMETER SIMULATIONS

For proper operation of a reflectometer system it is crucial that the reflected waves arrive at the receiver antenna. therefore, it is important to understand how the microwave beam is influenced by the plasma through which it propagates and how it is reflected from a curved and/or tilted reflection layer. Electron density, temperature, and magnetic field gradients in the plasma can refract the microwave beam in such a way that the reflected beam does not come back to the receiver antenna which is conventionally located close to the launching antenna. The alignment between the reflection layer and the microwave beam is also very important, especially when the distance between the reflection layer and the receiving antennas is large as is the case for ITER. A small misalignment already steers the reflected beam away from the receiving antenna and the signal is lost.

We have studied the effect of the curved flux surfaces for four selected frequencies, 135, 153, 158, and 190 GHz. The reflection layers for those frequencies are shown in figure 5. The 135 GHz reflection layer is very close to the low-field side edge, it is convex, and relativistic corrections are negligible because of the low edge electron temperature. After taking into account the relativistic corrections, the 153 and 158 GHz reflection layers become concave near the mid-plane, and they shift inward by 0.89 and 0.97 m at the height of the transmitter antenna, respectively, compared to the cold plasma reflection layers. The 190 GHz reflection layer shifts inward by 0.39 m and becomes slightly concave due to the relativistic effects.

In present-day experiments the shape of the reflection layer is usually convex due to a non-zero density gradient and "low" electron temperatures. Reflection from a convex reflection layer leads to a defocusing of the microwave beam and the reflected power is spread over significant range on the detector plane. (An example of such a conventional reflection is

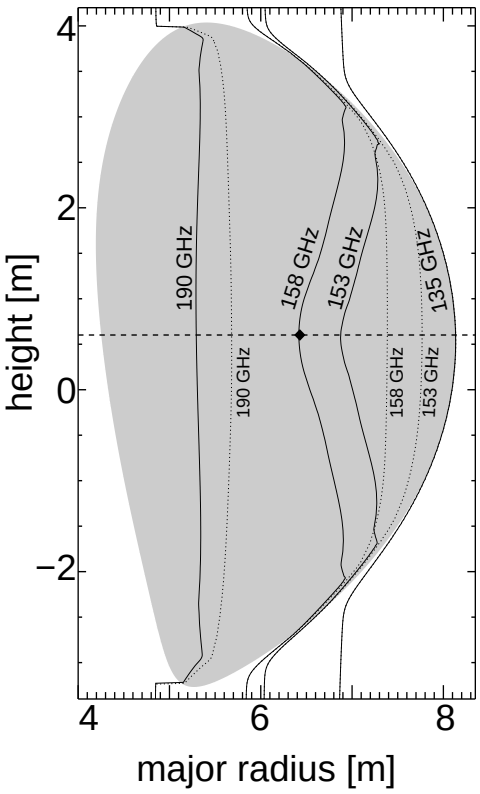

FIG. 5: Upper X-mode contours for the selected frequencies that are studied in detail.

shown in Fig. 1 of ref. [6]). In ITER, however, with its flat density profile and high and peaked electron temperature, the upper X-mode reflection layers are concave at the mid-plane over a large frequency range as shown in figure 4b. These concave reflection layers lead to a focusing of the reflected beam and also affect the spread of the microwave power as discussed next.

For the study of the focusing and alignment properties of the reflection layers we have performed simulations with the following parameters. For the four selected frequencies we have taken a Gaussian beam with a full width half maximum (FWHM) for the power of 9 cm and without beam divergence. The latter was taken in order to see clearly the (de)focusing effect due to the reflection layer in the plasma. The transmitter and receiver antennas were located at R=9.0 m which is 0.85 m away from last closed flux surface. We have moved our transmitter antenna from 10 cm below to 10 cm above the plasma mid-plane which is at 59.26 cm, in steps of 1 cm and recorded the reflected signal at the detector plane. Even though the 2-D code that was used is very fast, each calculation took between 3 minutes and

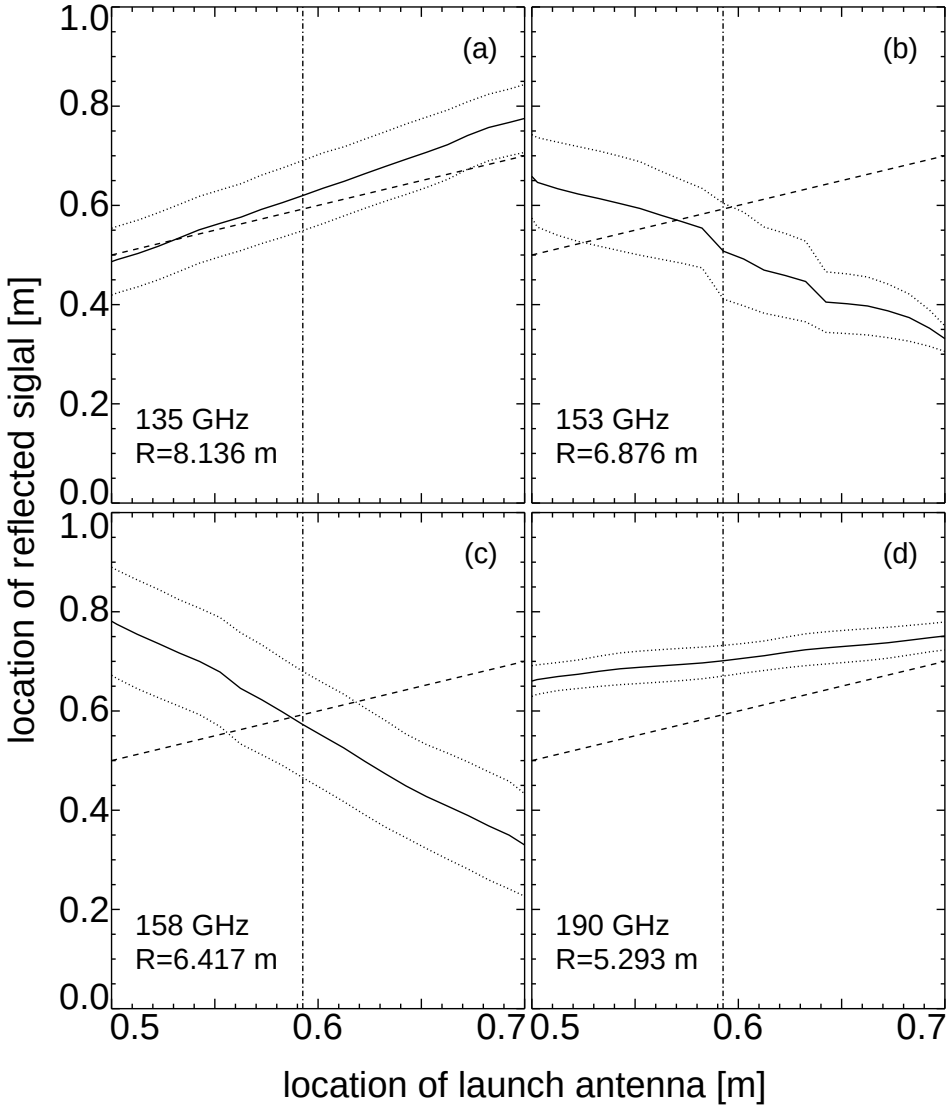

FIG. 6: Location of the maximum (solid line) reflected signal as a function of the position of the launch antenna for (a) 135 GHz, (b) 153 GHz, (c) 158 GHz, and (d) 190 GHz. At the dotted lines the signal has decreased to 50% and the dashed line indicate the center of the receiver antenna for the case when the receiver antenna is mounted next to the the transmitter antenna. The vertical dash-dotted lines indicate the plasma mid-plane.

10 hours of CPU time on a 2.4 GHz AMD Opteron dual processor machine with 16 Gb of memory running Redhat Linux. The long CPU times were due to the large computational domains used in some of simulations which were dictated by the large size of ITER and the curvature of the reflection layers. The computational region in the simulations was divided

into a region with free-wave propagation between the antennas and the plasma edge, a paraxial region between the edge and close to the reflection layer, and a full-wave region that covers the reflection layer [3]. For each of those regions the radial grid was optimized for computational speed: in the paraxial region two radial grid points per vacuum wave length were used while in the full wave region twenty radial grid points per vacuum wave length were used. In the vertical direction four points per vacuum wave length were used. This resulted for the 158 GHz simulations in a radial paraxial grid of 2200 points and a full wave grid of 700 points while there were 5100 grid points in the vertical direction.

Results of our simulations are shown in Fig. 6 where we have plotted the location of the maximum reflected signal, and the corresponding -3 dB points as a function of the transmitter location. The center of the receiver antenna for the case when the receiver antenna is mounted next to the the transmitter antenna as is currently proposed for the ITER low-field side reflectometer system is indicated as a dashed line in Fig. 6.

From Fig. 6a it can be seen that for the edge-localized reflection with a frequency of 135 GHz the reflected signal returns back to the transmitter location and the FWHM has increased from 9 to 14 cm, showing the defocusing due to the convex reflection layer.

The reflection of 153 GHz from a concave reflection layer shows some interesting features (Fig. 6b). When the waves are launched below the mid-plane the reflected beam at the detector plane has spread to 19 cm FWHM while launching the waves 10 cm above the mid-plane the FWHM has decreased to less than 5 cm. The concave curvature of the reflection layer focuses the reflected waves in the plasma. Moving along the reflecting surface from 10 cm below to 10 cm above the mid-plane changes the focus from 30 cm to 120 cm in front of the reflection layer and hence the spread of the reflected signal at the detector plane decreases. Not only the width of the reflected beam changes with launch position but also the location of the maximum signal as can be seen in Fig. 6b. This is due to a small tilt of reflection layer. A receiver antenna that is mounted next to the transmitter antenna will not detect the reflected signal when the transmitter-receiver antenna pair is away from the plasma mid-plane.

The vertical range over which a reflected signal returns to the launch location is even smaller for the 158 GHz channel (Fig. 6c). The reflection of 158 GHz comes from a layer that is located 1 cm beyond the plasma center. The FWHM of the reflected 158 GHz beam is 22 cm and it is independent of the vertical position, indicating that the curvature of this

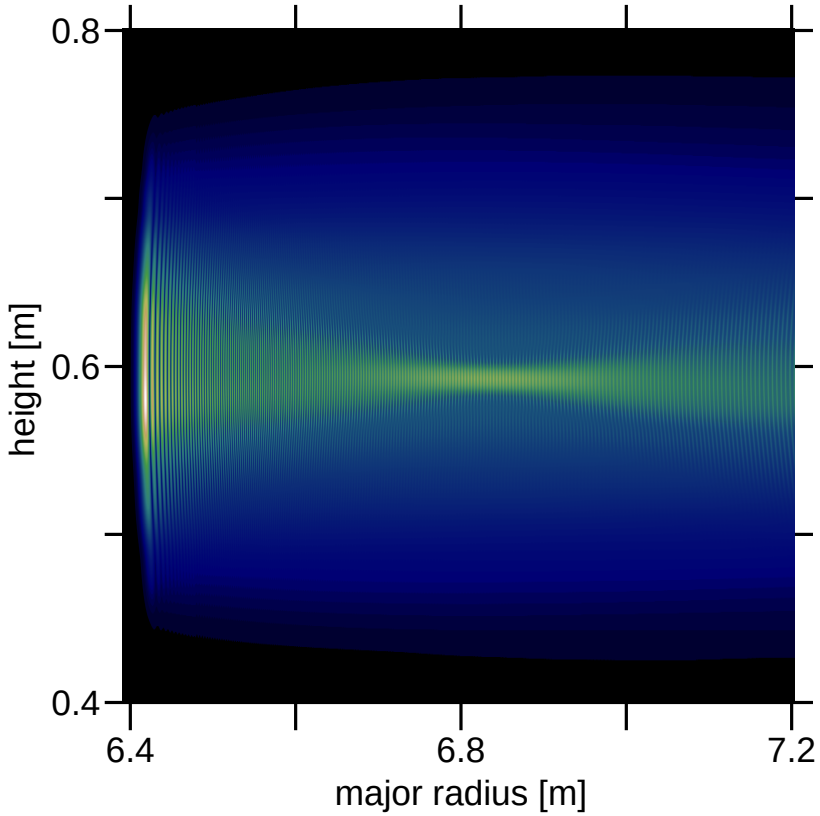

FIG. 7: The square root of the electrical field power for the 158 GHz full-wave solution at the cut-off (left) and the focus that is formed due to the concave curvature of the reflection layer. The intensity from low to high is indicated from black, blue, green, yellow, to white.

reflecting layer is constant. The 158 GHz reflected beam has a focus in the plasma which is located 44 cm in front of the reflection layer as can be seen in Fig. 7.

Because the ITER plasma shape is not up-down symmetrical due to the lower X-point at the divertor, the reflection layers at the high-field side are tilted slightly with respect to the vertical. This steers the reflected 190 GHz beam well away from its launch point as can be seen in Fig. 6d. The curvature at the 190 GHz layer is such that the FWHM of the reflected beam is reduced to 6 cm from the initial 9 cm at the launch antenna.

From the simulations presented above it is clear that the alignment of the reflectometer system with the plasma mid-plane is very important for detecting the reflected signals, especially for reflections deeper in the plasma and away from the low-field side edge. It is expected that the plasma mid-plane in ITER is not fixed but it will vary with different plasma scenarios. The design for the low-field side reflectometer system needs to have enough

built-in flexibility to cope with reflected signals that do not return to their launch point. In the next section we discuss some of the techniques to obtain such a flexibility.

V. ANTENNA SYSTEM

In the simulations so far we have used a parallel microwave beam without any divergence. This beam was chosen to clearly see the effects of the reflection layer curvature and reflection layer angle on the returned signals. One way to broaden the reflected wave distribution at the antenna plane is to launch a divergent microwave beam. In this way some of the power can return to the location of the receiver antenna. The effect of spreading the incident beam, launched at the plasma mid-plane, on the width of the reflected beam is shown in Fig. 8 for 135, 158, and 190 GHz. From this figure it can be seen that making a divergent beam spreads the reflected power over a much wider area on the detector plane, especially for the frequencies that probe the plasma core.

The disadvantage of spreading the reflected beam power over a wider area is that the reflected power that is detected with the receiver antenna approaches the noise background. Even if the launched microwave beam has a significant spread there are plasma scenarios possible with the plasma mid-plane displaced well above or below the plane defined by the reflectometer. In those cases the reflected signals still miss the receiver antenna even though the incident beam has a significant spread.

A second option to make the reflected signal return to a receiver antenna situated next to the transmiter antenna is by using steerable antennas. There are two good reasons to reject this idea. First, it complicates the hardware inside the port plug close to the plasma by introducing moving parts. Second, it might not be possible to steer the antennas to such a position that all the launched frequencies return to the receiver antenna. Third, steerable antennas are incompatible with ultrafast frequency sweep techniques for measuring density profiles [14].

A third option to detect reflected signals is to use a vertical array of receiver antennas. Antennas can be very robustly built, mounted near the plasma and the microwave signals can be transported without problems to a region behind the biological shield where they can be detected and processed separately for each receiver antenna. With an array of receiver antennas it is quite possible to detect the reflection from all the launched frequencies under

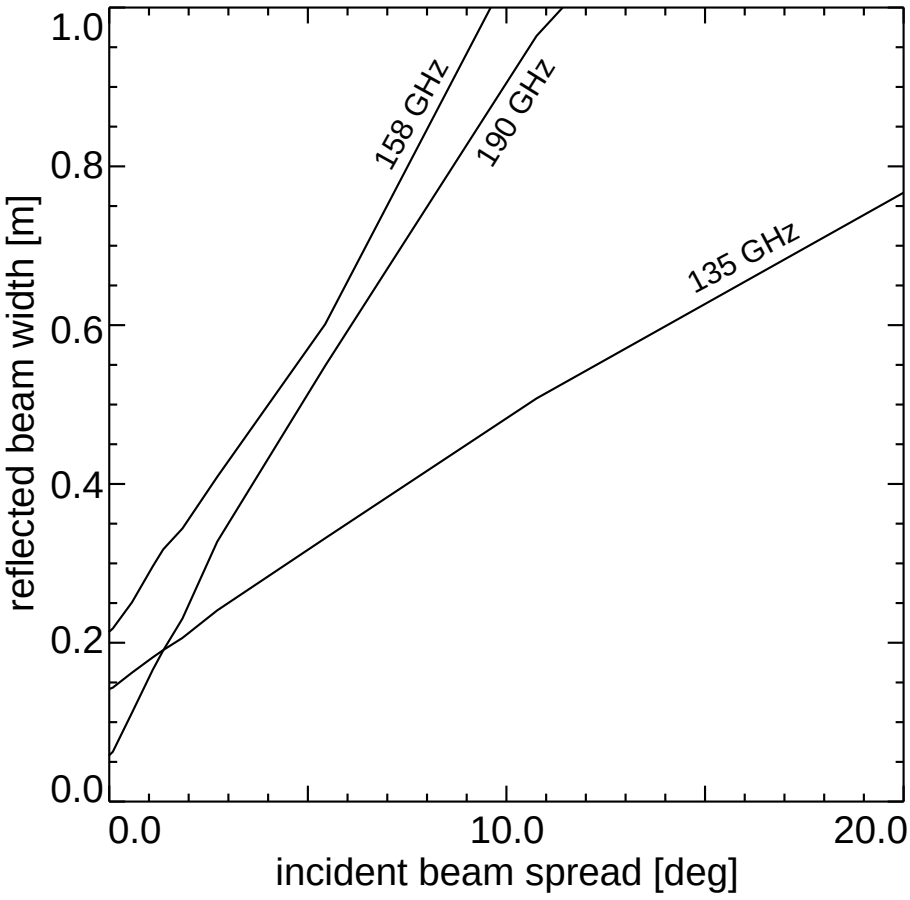

FIG. 8: The reflected beam width, defined as the distance between the -3 dB contours left and right from the maximum reflected power, as function of the incident spread, defined as the angle between the -3 dB contours left and right from the maximum incident power, for 135, 158, and 190 GHz microwave beams launched at the plasma mid-plane.

most plasma shapes and conditions. The drawbacks, however, are that each receiver antenna should have its own detector and that a waveguide run is needed from each of the receiver antennas to its detector.

An additional advantage of a poloidal receiver antenna array is that poloidal velocity measurements of the density turbulence can be made without much effort. By taking the cross correlation between the signals from two adjacent antennas the phase velocity of the scattered electrical field can be obtained. This velocity can then be related to the poloidal turbulent velocity via 2-D modeling. This technique was applied successfully on DIIID where a good agreement between poloidal velocities from charge exchange spectroscopy and

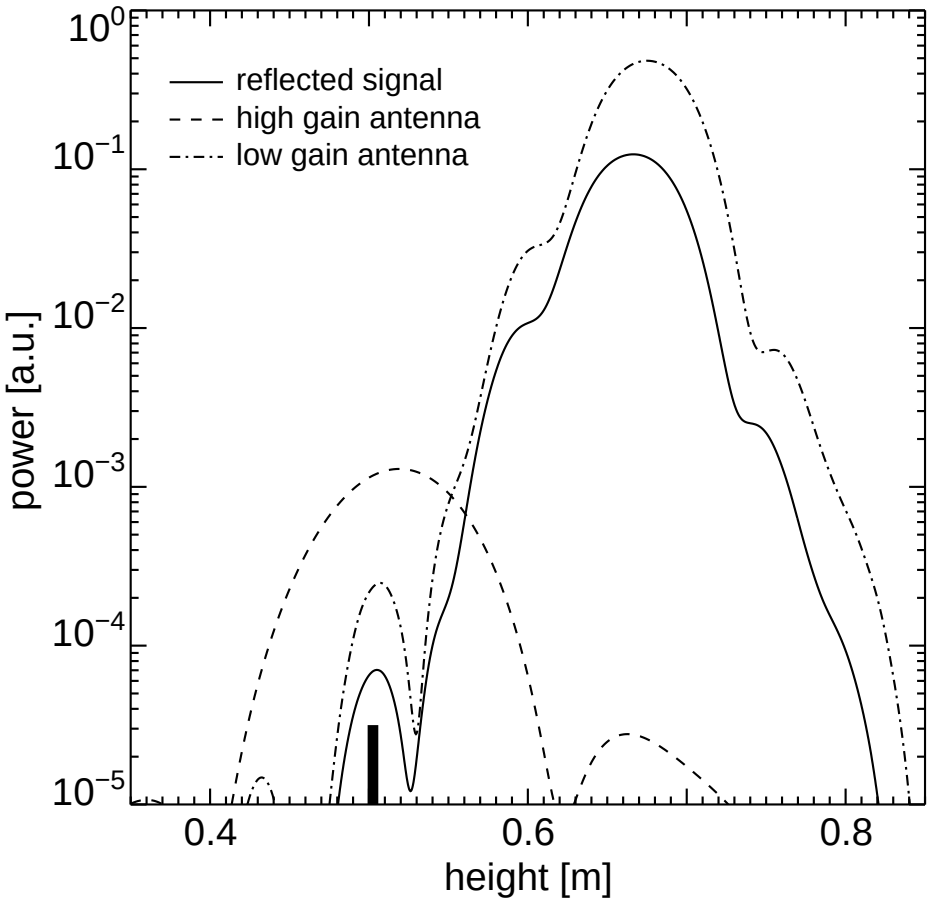

FIG. 9: The power of the 190 GHz reflected signal at the detector plane (solid line) folded with i) a high-gain antenna (dashed line) with an acceptance angle of 0.1 deg and ii) a low-gain antenna (dash-dotted line) with an acceptance angle of 21 deg. The location of the transmitter antenna is indicated with the solid bar at 0.5 m.

poloidal correlation reflectometry was obtained [15].

In current reflectometer systems the transmitter and receiver antenna are often chosen to be identical. This might not be the optimal choice for a poloidal receiver antenna array on ITER. A strong reflected signal is obtained by keeping the ingoing beam as narrow as possible which means that the transmitter antenna should be a high gain antenna. With the receiver antennas one wants to collect the reflected radiation from a wide range of angles. This requires a low gain antenna as illustrated in Fig. 9 where we have folded the reflected 190 GHz signal that was launched 10 cm below the plasma mid-plane with two different receiving antennas and calculated the antenna output as a function of the antenna location.

For this study We have used again a transmitter antenna beam with a 9 cm wide Gaussian beam without any spread. The first receiver antenna with a 9 cm Gaussian beam pattern at the antenna opening, had a high gain and hence a small acceptance angle of only 0.1 deg. and was aligned horizontally. This antenna only detects the small power near the launch antenna at 0.5 m but misses the strong reflection near 0.68 m due to its high directivity. On the other hand, the low-gain antenna with a 9 cm Gaussian beam pattern at the antenna opening and an acceptance angle of 21 deg., sees the strong reflected signal at 0.68 m. So, for a receiver antenna array it would be advantageous to use low-gain antennas with a wide acceptance angle.

The convex toroidal shape of the reflection layer spreads the reflected power in the toroidal direction and the received power will be less than the power calculated from a 2-D code. Due to the toroidal symmetry of the tokamak, the 2-D calculations of the power as presented here are qualitatively accurate but 3-D calculations that include absorption are needed for accurate quantitative estimates of received power levels. Nevertheless, it is clear from the 2-D calculations that only a low-gain wide-acceptance antenna is able to detect the reflected signal when it does not return back to the transmitter antenna.

VI. CONCLUSIONS

We have studied the response of the ITER low-field side reflectometer system where we have used the upper X-mode cut-off to probe a number of locations ranging from the low-field side edge to the halfway radius on the High-field side of the magnetic axis. For this study we have used a realistic 2-D ITER equilibrium of an ITER hybrid scenario with a constant electron density and a peaked electron temperature profile. It was found that the absorption of the microwave power due to the high electron temperatures is negligible for reflections off upper X-mode cut-off layers between the low-field plasma edge and beyond the plasma center. As was found before [13] the reflection layer locations can shift by almost one meter compared to the cold-plasma approximation due to relativistic corrections. This shift has important consequences for low field side reflectometry on ITER as identified in this paper. The peaked electron temperature profile created concavely curved reflection layers near the plasma center. These concave reflection layers can form a focus for the reflected beam and create a smaller reflected beam at the detector plane than was launched into the

plasma. In the simulations it was also found that the reflected beam does not always return to the launch location. This is caused by a slight tilt of the reflection layers at the mid-plane due to ITER's highly asymmetric up-down plasma shape. In order not to miss the reflected signal under different ITER plasma scenarios, we propose to further design and install a poloidal array of low-gain receiver antennas with a wide acceptance angle instead of a small number of transmitter-receiver antenna pairs. The transmitter antenna (or antennas) should be highly collimated for an optimal signal to noise ratio.

Acknowledgments

This work has been conducted under DOE Contract No. DE-AC02-76-CH0373.

[1] G. Vayakis, T. Ando, N. Bretz, L. de Kock, A.J.H. Donné, E.J. Doyle, J. Irby, E. Martin, M. Manso, A. Mase, J. Sanchez, V.A. Vershkov, D. Wagner, C.I. Walker, and the ITER Joint Central Team and Home teams, Diagnostics for Experimental Thermonuclear Fusion Reactors 2, Edited by P.E. Stott, G. Gorini, P. Prandoni and E. Sindoni, Plenum Press, New York, 97 (1998).

[2] G. Vayakis et al., Status and prospects for mm-wave reflectometry in ITER, Submitted to Nucl. Fusion.

[3] E.J. Valeo, G.J. Kramer, and R. Nazikian, Plasma Phys. Contr. Fusion **44** L1 (2002).

[4] G.J. Kramer, R. Nazikian, and E.J. Valeo, Plasma Phys. Contr. Fusion **44** L11 (2002).

[5] G.J. Kramer, R. Nazikian, and E.J. Valeo, Rev. Sci. Instrum. **74** 1421 (2003).

[6] R. Nazikian, K. Shinohara, G.J. Kramer, E. Valeo, K. Hill, T.S. Hahm, G. Rewoldt, S. Ide, Y. Koide, Y. Oyama, H. Shirai, and W. Tang, Phys. Rev. Lett. 94, 135002 (2005)

[7] S.C. Jardin, N. Pomphrey, and J. DeLucia, J.Compt. Phys. **66** 481 (1983)

[8] J.E. Kinsey, G.M. Staebler, and R.E. Waltz, Phys. Plasmas **12** 052503 (2005).

[9] R.V. Budny, M.G. Bell, A.C. Janos, D.L. Jassby, L.C. Johnson, D.K. Mansfield, D.C. McCune, M.H. Redi, J.F. Schivell, G. Taylor, T.B. Terpstra, M.C. Zarnstorff, and S.J. Zweben, Nucl. Fusion **35**, 1497 (1995).

[10] I.P. Shkarofsky, J. Plasma Physics **35** 319 (1986).

[11] H. Bindslev, Plasma Phys. Contr. Fusion **35** 1093 (1993)

[12] D.B. Batchelor, R.C. Goldfinger, and H. Weitzner, Phys. Fluids **27** 2835 (1984).

[13] H. Bindslev, Plasma Phys. Contr. Fusion **34** 1601 (1992)

[14] Ph. Moreau, F. Clairet, J.M. Chareau, M. Paume, and C. Laviron, Rev. Sci. Instrum. **71** 74 (2000).

[15] T.N. Carlstrom, R.J. Groebner, C. Fenzi, G.R. McKee, R.A. Moyer, and T.L. Rhodes, Plasma Phys. Contr. Fusion **44** A333 (2002) A quantitative analysis of the poloidal reflectometer data pesented in this paper was reported in G.J. Kramer, T.L. Rhodes, W.M. Solomon, G.R. McKee, R. Nazikian, E. Valeo, R.V. Budny, and W.A. Peebles, 45^{th} Annual Meeting of the American Physical Society Division of Plasma Physics, Albuquerque, New Mexico Oct. 27-31, GO1-14 130 (2003).

External Distribution

Plasma Research Laboratory, Australian National University, Australia
Professor I.R. Jones, Flinders University, Australia
Professor João Canalle, Instituto de Fisica DEQ/IF - UERJ, Brazil
Mr. Gerson O. Ludwig, Instituto Nacional de Pesquisas, Brazil
Dr. P.H. Sakanaka, Instituto Fisica, Brazil
The Librarian, Culham Science Center, England
Mrs. S.A. Hutchinson, JET Library, England
Professor M.N. Bussac, Ecole Polytechnique, France
Librarian, Max-Planck-Institut für Plasmaphysik, Germany
Jolan Moldvai, Reports Library, Hungarian Academy of Sciences, Central Research Institute for Physics, Hungary
Dr. P. Kaw, Institute for Plasma Research, India
Ms. P.J. Pathak, Librarian, Institute for Plasma Research, India
Dr. Pandji Triadyaksa, Fakultas MIPA Universitas Diponegoro, Indonesia
Professor Sami Cuperman, Plasma Physics Group, Tel Aviv University, Israel
Ms. Clelia De Palo, Associazione EURATOM-ENEA, Italy
Dr. G. Grosso, Instituto di Fisica del Plasma, Italy
Librarian, Naka Fusion Research Establishment, JAERI, Japan
Library, Laboratory for Complex Energy Processes, Institute for Advanced Study, Kyoto University, Japan
Research Information Center, National Institute for Fusion Science, Japan
Professor Toshitaka Idehara, Director, Research Center for Development of Far-Infrared Region, Fukui University, Japan
Dr. O. Mitarai, Kyushu Tokai University, Japan
Mr. Adefila Olumide, Ilorin, Kwara State, Nigeria
Dr. Jiangang Li, Institute of Plasma Physics, Chinese Academy of Sciences, People's Republic of China
Professor Yuping Huo, School of Physical Science and Technology, People's Republic of China
Library, Academia Sinica, Institute of Plasma Physics, People's Republic of China
Librarian, Institute of Physics, Chinese Academy of Sciences, People's Republic of China
Dr. S. Mirnov, TRINITI, Troitsk, Russian Federation, Russia
Dr. V.S. Strelkov, Kurchatov Institute, Russian Federation, Russia
Kazi Firoz, UPJS, Kosice, Slovakia
Professor Peter Lukac, Katedra Fyziky Plazmy MFF UK, Mlynska dolina F-2, Komenskeho Univerzita, SK-842 15 Bratislava, Slovakia
Dr. G.S. Lee, Korea Basic Science Institute, South Korea
Dr. Rasulkhozha S. Sharafiddinov, Theoretical Physics Division, Insitute of Nuclear Physics, Uzbekistan
Institute for Plasma Research, University of Maryland, USA
Librarian, Fusion Energy Division, Oak Ridge National Laboratory, USA
Librarian, Institute of Fusion Studies, University of Texas, USA
Librarian, Magnetic Fusion Program, Lawrence Livermore National Laboratory, USA
Library, General Atomics, USA
Plasma Physics Group, Fusion Energy Research Program, University of California at San Diego, USA
Plasma Physics Library, Columbia University, USA
Alkesh Punjabi, Center for Fusion Research and Training, Hampton University, USA
Dr. W.M. Stacey, Fusion Research Center, Georgia Institute of Technology, USA
Director, Research Division, OFES, Washington, D.C. 20585-1290

The Princeton Plasma Physics Laboratory is operated
by Princeton University under contract
with the U.S. Department of Energy.

Information Services
Princeton Plasma Physics Laboratory
P.O. Box 451
Princeton, NJ 08543

Phone: 609-243-2750
Fax: 609-243-2751
e-mail: pppl_info@pppl.gov
Internet Address: http://www.pppl.gov